Journal of Porous Materials (2023) 30:1337–1356
https://doi.org/10.1007/s10934-023-01425-3

Synthesis and characterization of polyurethane rigid foam by using feedstocks received from renewable and recyclable resources

Muntajab Sarim[1] · Mir Mohammad Alavi Nikje[1] · Maryam Dargahi[1]

Published online: 7 February 2023

Abstract
The mimicry reactions used in the industrial field based on pure materials to obtain products is very important in order to achieve a circular economy and a green environment. This time around, the idea is that all raw materials are wastes. In addition to synthesizing biodiesel, this study aims to synthesize polyurethane rigid foams from recyclable materials such as liquid wastes and solid plastic wastes. The study follows preparation of a new class of biopolyols by reacting a mixture of crude glycerin-based polyol and epoxidized used cooking oil with polyethylene terephthalate, polyurethane, and bisphenol-polycarbonate wastes. Then, fabrication of polyurethane rigid foams by blending synthesized biopolyols with commercial polyol at ratios 20%, 40%, and 60% occurs. The properties of biopolyols and fabricated rigid foams was investigated by nuclear magnetic resonance, infrared spectrometer, thermal gravimetric analyzer, scanning electron microscope, and dynamic mechanical thermal analyzer. The results show that the biopolyols are valuable products for polyurethane manufactures. Moreover, the fabricated rigid foams show nonsignificant changes at the commercial and industrial level.

Keywords Polyurethane rigid foam · Used cooking oil · Crude glycerin · Polyethylene terephthalate wastes · Polyurethane wastes · And Bisphenol-polycarbonate wastes

Abbreviations

BD	Biodiesel
BPA	Bisphenol-A polycarbonate
CG	Crude glycerin
Com. G	Commercial Glycerin
DEG	Diethylene glycol
EUO	Epoxidized used cooking oil
MNPs	Magnetic nanoparticles
PGL	Polyol of crude glycerin
PET	Polyethylene terephthalate
PU	Polyurethane
PURF	Polyurethane Rigid foam
UCO	Used cooking oil

1 Introduction

Crude oil is the basis of the raw components for polyurethane production, and this reality suffers from many problems such as insufficient raw materials and price stability, in addition to being dangerous chemical with gaseous emissions that contribute to increasing global warming. This reality is not only related to the polyurethane industry but also goes beyond that to include all petrochemical industries [1–3]. Recently, due to the strict green chemistry rules and environmental concerns, natural raw ingredients such as vegetable oils have become the future destination of most industries not only, they are abundant, sustainable, and biologically derived, but also, they are environmentally friendly [4–6]. On the other hand, in addition to the petrochemical crisis resulting from the low level of oil in the earth's crust, the COVID-19 pandemic has disrupted the global supply chain from the countries with the largest oil refining capacity, namely the United States of America, China and Russia. This crisis exposed the weaknesses and imbalances of the economies of other countries, prompting researchers to focus more on developing new materials that are more sustainable and more capable of being locally manufactured [7–10].

✉ Mir Mohammad Alavi Nikje
alavi@sci.ikiu.ac.ir

Muntajab Sarim
muntajabsarim@gmail.com

Maryam Dargahi
dargahi@sci.ikiu.ac.ir

[1] Department of Chemistry, Faculty of Science, Imam Khomeini International University (IKIU), Qazvin, Iran

A series of complex reactions occur while frying food such as oxidation, hydrolysis, isomerization, and polymerization which affect the chemical composition of the oil. These reactions produce a number of products including volatile compounds, hydrolyzed products, oxidized triacylglycerol monomers, cyclic compounds, trans-configuration compounds, polymers, sterol derivatives, heterocyclic compounds containing nitrogen and sulfur, acrylamide...etc. Outputs are affected by various factors such as type of frying oil, frying conditions, and type of fried material. UCO leads to problems in the sewage network and poisoning of treatment [11–13]. Some studies indicate that they have identified some properties of inedible UCO collected from different restaurants. Hydroxyl numbers ranged from 1.0 to 5.0 mg KOH/g, acid values ranged between 1.5 and 5.2 mg KOH/g, iodine values ranged 105.7–111.9 g/100 g, viscosity values 59.0–71.0 mPa.s, polycyclic aromatic hydrocarbons (PAHs) 25.1–118.0 µg/kg, and polychlorinated biphenyls (PCBs) 3.5–69.1 µg/kg [14]. The values indicate that UCO is unfit for human consumption and at the same time a simple modification can be made to change the properties and make these types of materials more valuable. Indeed, the recent increase in the number of publications and patents confirms the huge potential that UCO has—when recycling—beyond its use only in the production of BD as it can be used as valuable chemicals [9, 15, 16].

Despite the high characteristics of BD based on vegetable oils, which make it a promising alternative to conventional fuels, this process is not economically feasible due to the high price of reactants. Thus, the price of BD is 1.5 times higher than that of conventional fuels. More, the use of homogeneous catalysts increases the cost of the production process. It should be noted here that the acid catalysts are superior to the alkaline catalysts by not forming soaps in the reaction products. Therefore, it was necessary to make this process more economical, and UCOs have been given the most attention for this reason. Besides, acid solid catalysts were adopted as environmentally friendly catalysts [10, 17–22].

BD is often highlighted as the main product of the transesterification process of vegetable oils, but companies are also interested in the main by-product, which is crude glycerin CG (100.0 kg BD:10.0 kg CG). The CG has major impurities such as water, methanol, and mono- and di- acyl glycerides in small amounts. The use of CG in many industries requires that it be available in high purity and therefore requires the use of various purification processes. Studies have shown that the purification treatments are uneconomical feasibly. From here, the search has begun for the inclusion of CG in other industries, the most important of which is polyurethane [23, 24]. Luo and Li have produced polyols and PU foams using PET and CG mediated DEG. The polyols have hydroxyl number between 282.6 and 439.6 mg KOH/g with viscosities 658.0 and 4994.0 mPa.s whereas the foams exhibited apparent densities between 0.025 and 0.029 g/cm^3 and compressive strength between 86.4 and 179.5 kPa [25].

Also, EUO can be obtained from the reaction of UCO with percarboxylic acids in the presence of homogeneous catalysts such as sulfuric acid and phosphorous acid, or heterogeneous catalysts, such as sulfuric ion exchange resins and sulfonated metal oxides. MNPs catalysts were present in the process of epoxidation of double bonds of vegetable oils. For example, an amphiphilic compound was synthesized with a magnetic core and a dodecyl amine-modified polyoxometalate-paired poly- (ionic liquid) shell. This catalyst exhibits high activity and selectivity, along with suitable magnetic recovery and efficient regeneration [26].

Environmentally polyols, which are named biopolymers, can be obtained from either transesterification of oils or ring-opening of epoxidized oils processes by using a wide range of reactive materials such as alcohols in wide ranges of hydroxyl numbers as well functionalities and viscosities. Regarding ring-opening of EUO with diethylene glycol, the hydroxyl number was 139.6 and 159.2 mg KOH/g with viscosities 3275.0 and 961.0 mPa.s by using two types of catalysts namely, tetrafluoro boric acid and sulfuric acid. As for the transesterification of UCO with agents such as ethylene glycol, propylene glycol, diethylene glycol, glycerin, and triethanolamine, concluded that alcohols containing two primary hydroxyl groups were more reactive than alcohols containing three hydroxyl groups or two hydroxyl groups including one primary and one secondary group and the most reactive agent was triethanolamine. Maria and others have fabricated foams based on mixtures of commercial polyol with polyol from UCO (20, 40, 60, 80 and 100%). Increasing the biopolyol content (up to 60%) increased the closed cell content. More, foam with a content of 100% biopolyol has led to the open-cell foams. Apparent density ranged from 0.013 to 0.018 g/cm^3. The compressive strength and dimensional stability of most biofoams were distinguished by a value above the compressive strength of the reference material [15, 16].

PET, PU, BPA, PE, PP, PVC ...etc., are considered the most widely used due to their desirable properties, and their waste amount is directly proportional to the amount of their production, as make up more than 90% of the current plastic production. Since the production costs of these materials with regard to the level of its properties justify the recycling operations, the correlation between processing costs and the economy is much more advantageous than many other thermoplastics, so processes consisting of more than one step process are definitely worth it. Therefore, efforts are always made to find simpler, environmentally friendly, reasonable, and more economical processes than the known processes [27–29]. Recycling processes vary between

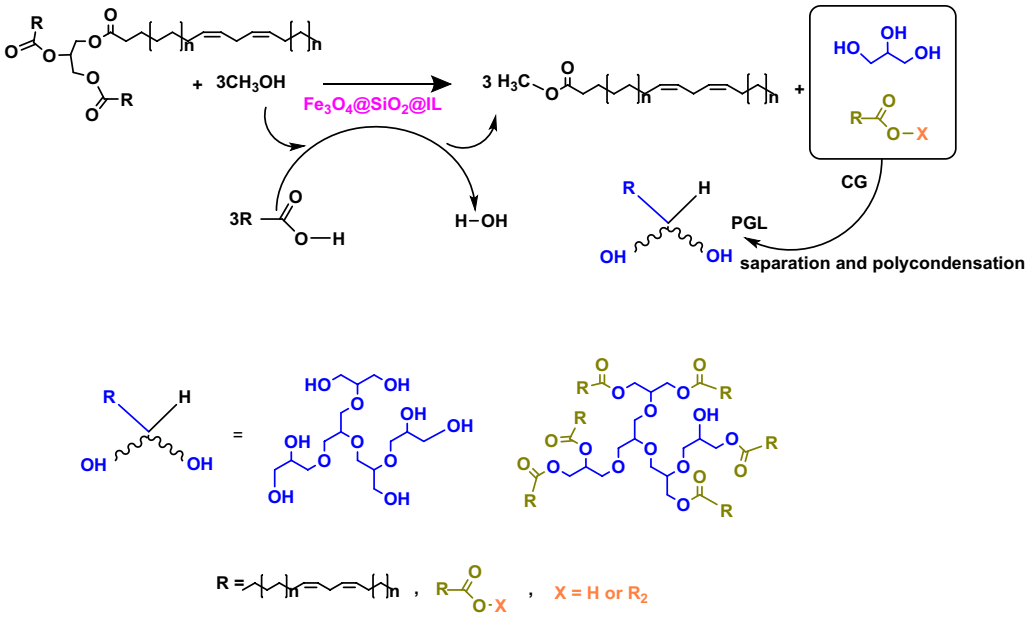

Fig.1 PGL synthesis

Fig. 2 Biopol-B synthesis

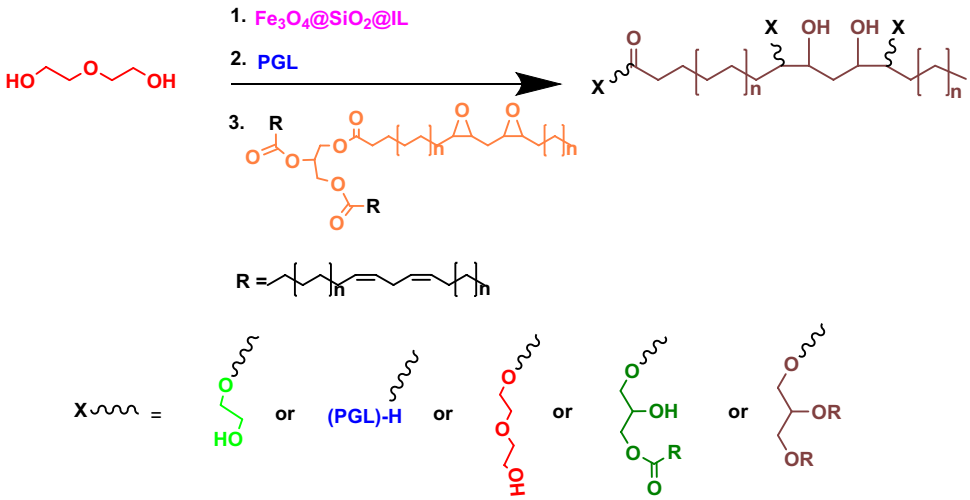

primary recycling (reuse or sorting), secondary recycling (or mechanical recycling), chemical recycling (or Feedstock), and quaternary recycling (or energy recovery). However, recently, chemical recycling has attracted interest due to the possibility of controlling the reaction and the ability to reach the target product by one or more of chemical reactions: Hydrogenation, Glycolysis, Gasification, Hydrolysis, Pyrolysis, Methanolysis…etc. One of the most important chemical recycling methods for PET, PU, and BPA wastes used on a commercial scale is glycolysis. The main product from this process is polyol, where the polyol recovered from the waste can be replaced by up to 50% of virgin polyol used in the manufacturing of polyurethane. To achieve more valuable polymers with terminal hydroxyl groups during the chemical recycling process of glycolysis, it is necessary to use a wide range of methods including various catalysts, different (monoary, binary and ternary) solvent systems such as (pentaerythritol, ethylene glycol, glycerin, glycerin/methylol propane, diethylene glycol/diethanolamine, glycerin/sorbitol/water). Patents interested in recycling plastic increased as the production increased. The most important of these inventions are those related to the production of rigid foams from an aromatic polyester polyol mixture. The polyols were obtained by reacting polyethylene terephthalate with alkylene glycol and forming a terephthalic ester product and then reacting the product with alkylene oxide to form an aromatic polyol product. The aim of these works was to produce aromatic polyester polyols to be used as an

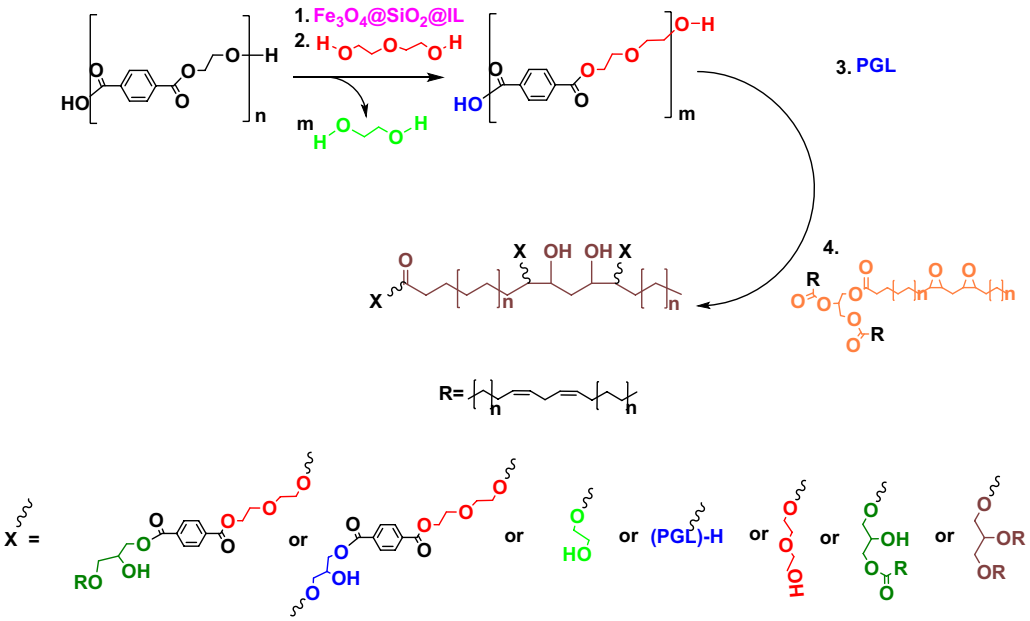

Fig. 3 Biopol-PET synthesis

Fig. 4 Biopol-PU synthesis

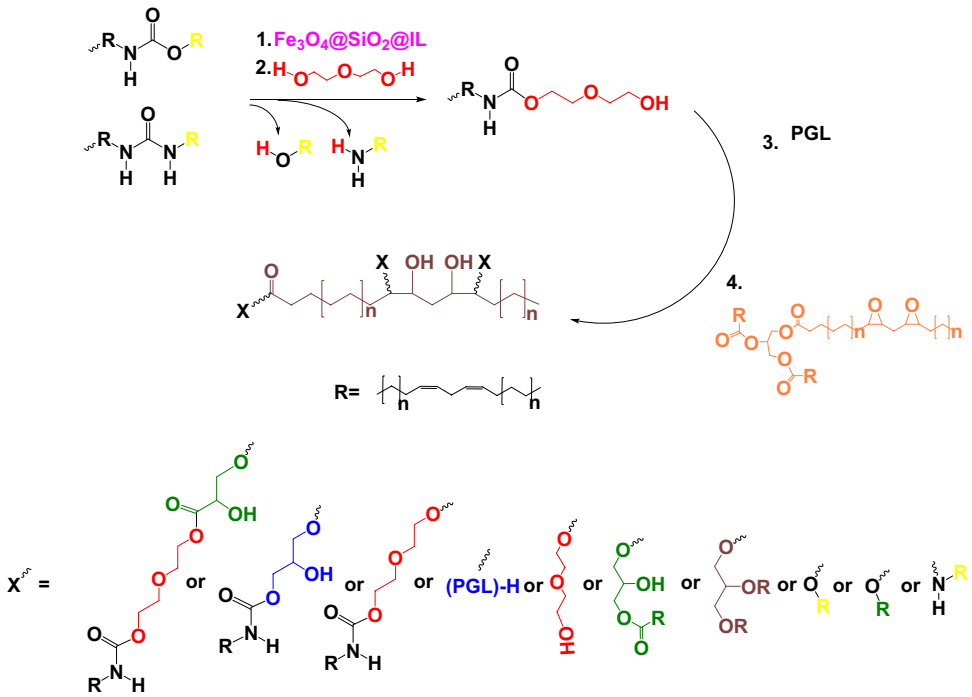

inexpensive alternative to the more expensive commercial polyols expanders. Recycled materials include scrap and flakes for PET, DMT...etc. Alkylene glycol includes ethylene glycol (EG), propylene glycol (1,2-propylene glycol), diethylene glycol (DEG), dipropylene glycol and triethylene glycol (TEG), ...etc. While alkylene oxides, propylene oxide appeared to be the most effective in this regard in addition to ethylene oxide and 1,2-butylene oxide. The main catalysts used are sodium and potassium hydroxide. Some patents talked about recycling polyurethane waste collected from car seats, furniture, sofas, cushions, upholstery or seats with a mixture of polyols to produce new classes of polyols with hydroxyl numbers between 35.0 and 650.0 mg KOH/g at temperatures between 170 and 210 °C. It was mentioned that the resulting polyol mixture contains very valuable and effective materials such as oligo-urea, polyurea, and

Fig. 5 Biopol-BPA synthesis

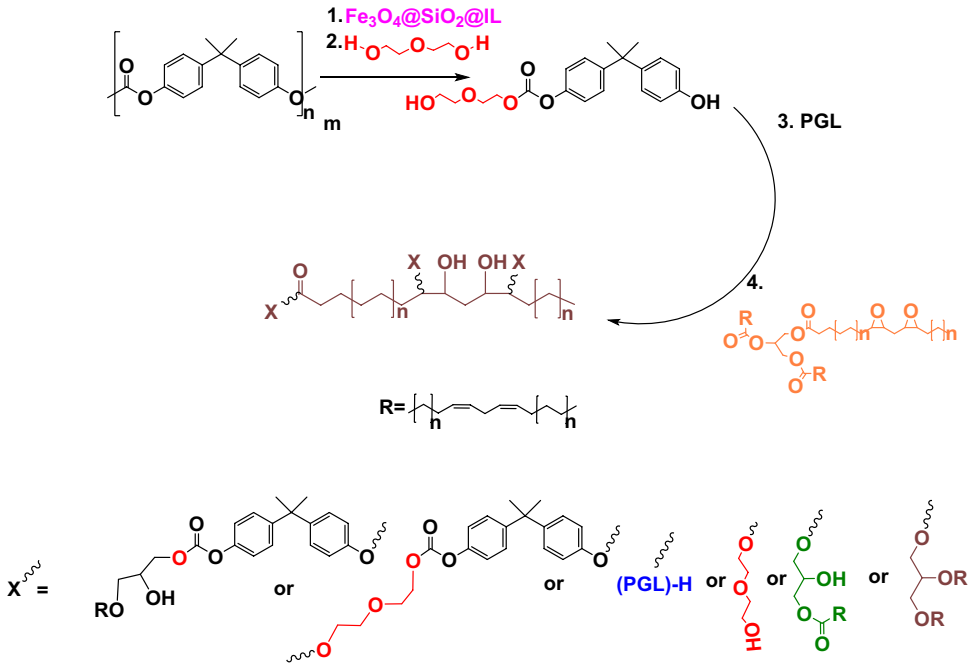

Table 1 Codes of prepared PURFs from commercial polyol and novel polyols with different ratios & Formulations of prepared foams

PURFs Code		$PU_{\_com}$	x	$PU_{\_x\text{-}20}$	$PU_{\_x\text{-}40}$	$PU_{\_x\text{-}60}$
A component	pbw Commercial polyol	100.0		80.0	60.0	40.0
	pbw Synthesized polyols	0		20.0	40.0	60.0
	CAT (AP CAT 28)				2.4	
	pbw foaming agent				0.2	
	pbw surfactant				0.2	
	pbw pentane				0.2	
B component	pbw MDI	136.1	1	152.4	148.7	144.9
			2	151.5	146.8	142.1
			3	150.9	145.7	140.4
			4	161.7	167.4	172.9

com: comparative sample or reference sample
x = 1, 2, 3, and 4 for novel biopolyols B, PET, PU, and BPA, respectively

Table 2 Characteristics of the PGL, EUO, and biopolyols

	PGL	Biopol-B	Biopol-PET	Biopol-PU	Biopol-BPA
OH value (mg KOH/g)	270 ± 30	160 ± 20	140 ± 20	128 ± 20	360 ± 40
Hydroxyl (%)	–	6.8	5.9	5.4	15.3
Acid value (mg KOH/g)	1.9	2.8	1.4	2.2	9.8
Carboxyl (%)	–	0.2	0.1	0.7	2.0
Viscosity average (mPa.s)	689.0	54.0	37.0	831.0	2519.0
Content of glycerol[a] in CG was 34.0%					

[a]The content of glycerol in CG was determined by the method[40]

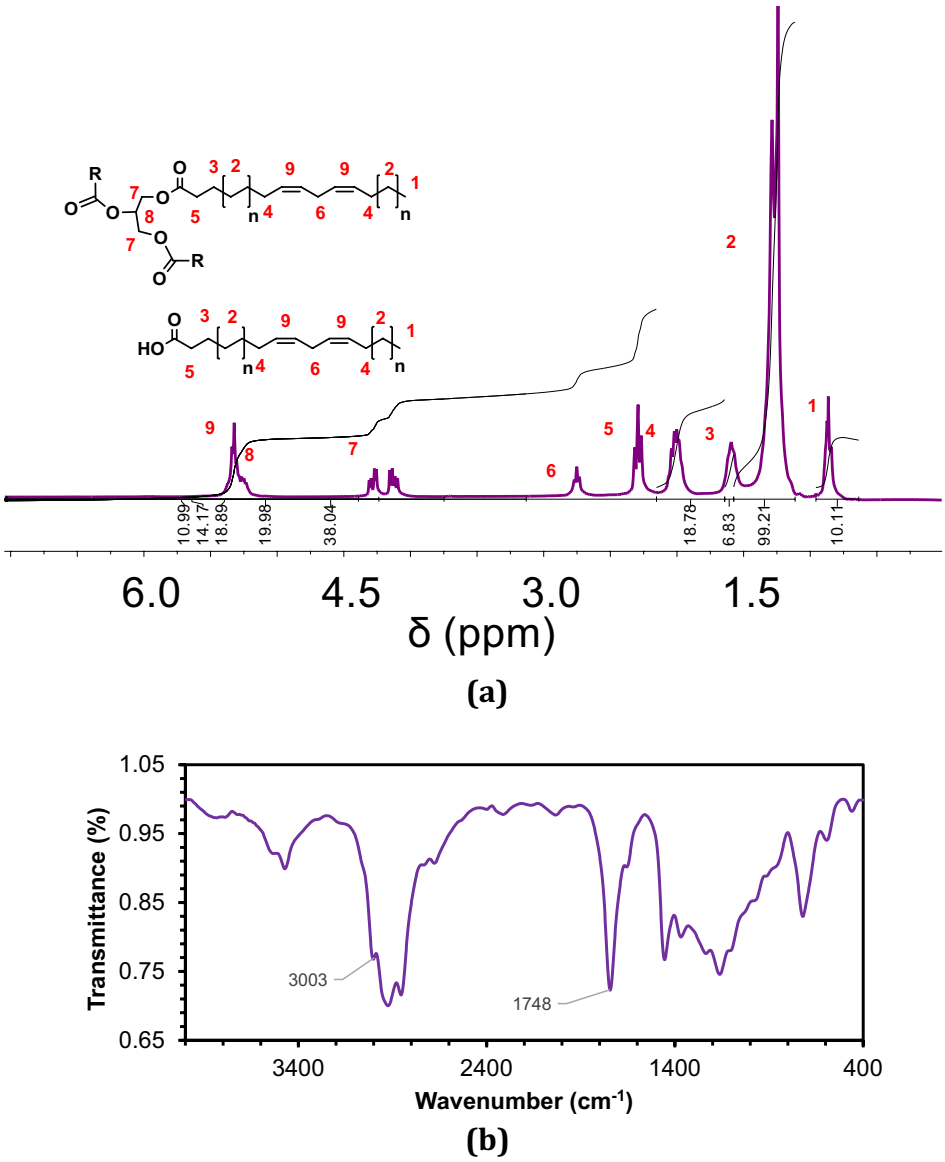

Fig. 6 ^{1}HNMR (**a**) and FTIR (**b**) of UCO

polyamides. The patents also include PC-BPA recycling where it is possible to condense granules of waste polycarbonate BPA in a vacuum with OH-terminal compounds directly and to produce polycarbonate with higher molecular weights using alkaline catalysts or phosphorous salts via a transesterification reaction [30–39].

For the first time, our study reported the usage of PGL and EUO from UCO in the recycling process separately of three wastes PET, PU, and BPA to produce new classes of biopolyols and blend partially (20%, 40%, and 60%) with a commercial polyol to produce PU foams. The recycling processes include first complete depolymerization of PET, PU, and BPA wastes in DEG, then reacting the depolymerized wastes with a heated mixture of PGL and EUO by using MNPs catalyst. The characteristics of biopolyols and fabricated foams are determined and investigated by using common operations and techniques.

2 Experimental

2.1 Materials

MERPESOL 146-\B2\PIR POLYOL, (Density: 1.1 ± 0.1 g/cm^3, Yellow Liquid Viscosity: 3200 ± 200 mPa.s at 25 °C, OH Number: 240 ± 20 mg KOH/g, Water content: 0.1%, Acid value: < 1.0 max mg KOH/g) was purchased from BAYER, Germany. Methylene diphenyl diisocyanate (MDI) Suprasec®5005, (Dark Brown Liquid, Viscosity: 220 mPa.s at 25 °C) was purchased from Huntsman, Germany. Diethylene glycol (Density:1.1 g/cm^3, Molecular Weight: 106.1 g/

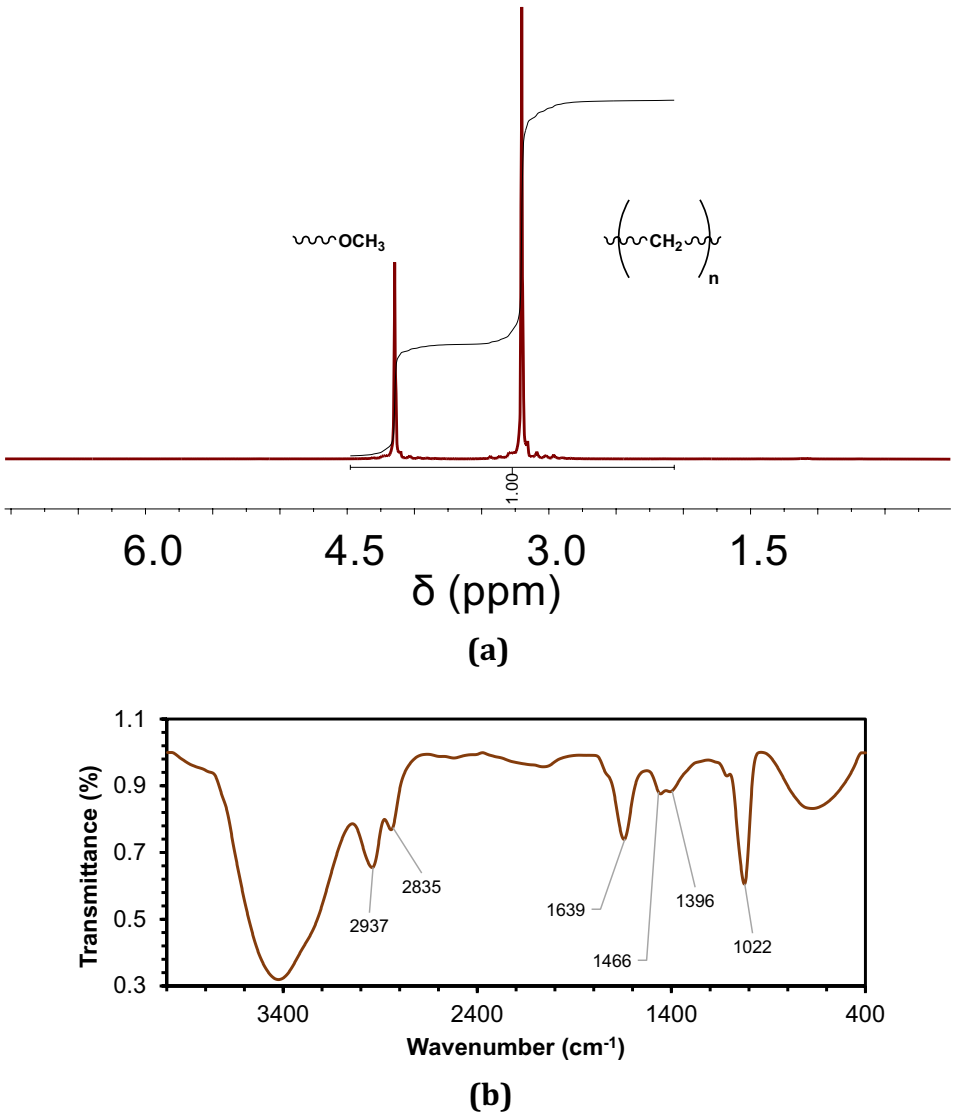

Fig. 7 [1]HNMR (**a**) and FTIR (**b**) of BD

mol) was purchased from Sigma Aldrich, USA. Used cooking oil (OH value 1.7 mg KOH/g, Yellow Liquid viscosity 67.0 mPa.s.), was collected from restaurants in Qazvin, Iran. Epoxized used cooking oil (OH value: 2.9 mg KOH/g, Acid value: 3.7 mg KOH/g, Viscosity average: 148.0 mPa.s). PET, PU, PC wastes were collected from Qazvin, Iran.

2.2 Instrument

FTIR spectra (400–4000/cm) was carried out on a Bruckner Tensor 27 spectrophotometer. [1]H-NMR spectra was performed in a Bruker 300 nuclear magnetic resonance instrument, using deuterated chloroform (DMSO or CDCl3) as solvent. Viscosity (η) was determined at 25 °C using a rotational rheometer (Rheolab QC, Anton Paar). TGA was done with Perkin-Elmer Pyris Diamond TG/DTA under air atmosphere at a heating rate of 10 °C/min. Dynamic Mechanical Thermal Analyzer, NETZSCH, Germany, temperature range: 25–250 °C, temperature rate: 10 °C/min, Frequency: 1 Hz. Scanning electron microscope, TESCAM MIRA III, Czech Republic.

2.3 PGL synthesis procedure

To obtain PGL, 100.0 g of UCO was placed in a refluxed three-necked round flask. 30.0 g of methanol and 1wt% catalyst was added for 6 h at 60 °C. Distilled water was added to the reaction product and the aqueous phase separated from the organic phase using a 250.0 mL separating funnel. The washing process was repeated several times to collect the aqueous phase and then the water was evaporated. The CG product was placed in the same flask with 1 wt% catalyst at 200 °C for 6 h under vacuum. The water and excess methanol were evaporated and separated, Fig. 1.

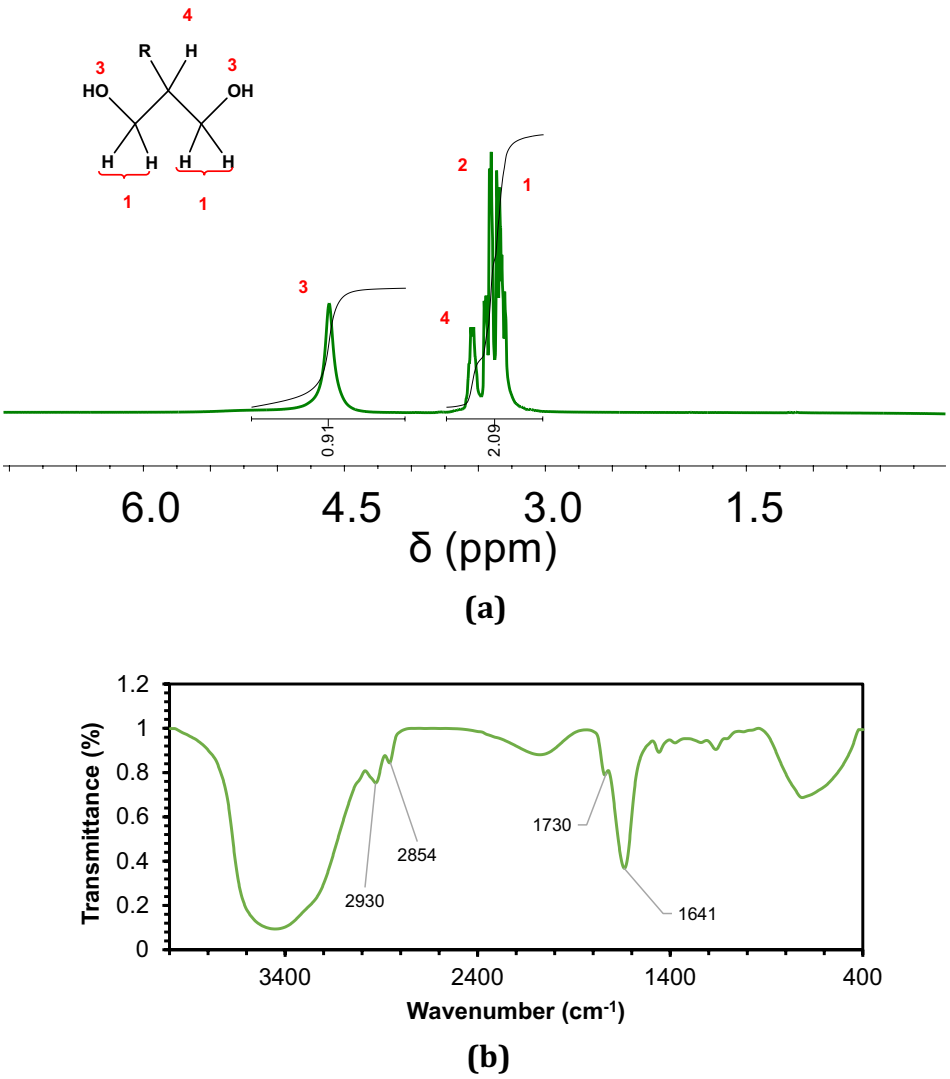

Fig. 8 [1]HNMR (**a**) and FTIR (**b**) of PGL

2.4 Novel biopolyols synthesis procedure

Four polyols were synthesized under the same conditions. The reactions were obtained in a 4 refluxed three-necked round flask, 20.0 g of diethylene glycol and 1% of catalyst were placed in the flask and heated to 200–205 °C. Intermittently, 10.0 g of the wastes PET, PU, and PC for biopol-PET, biopol-PU, and biopol-BPA were separately added (0.5 g/3 min). After complete dissolution of the wastes, a heated mixture (5:5) of PGL and EUO was gradually added. Biopol-B[1] was obtained at the same steps but without wastes, Figs. 2, 3, 4, 5.

2.5 Preparation of polyurethane rigid foams

The polyurethane rigid foams were carried out by a one-step process from A and B components. A component consists of polyols with different contents of novel biopolyols (0, 20, 40, and 60 wt%) for foams. B component (isocyanate) was added to the system, mixed mechanically in an open mold, and kept for 24 h at room temperature, Table 1.

[1] Biopol-B: Biopolyol Blank.

3 Results and discussion

3.1 Characterization of PGL, EUO, and biopolyols

The characteristics OH, acid, and functionality values of the EUO, PGL and biopolyols are determined according to [40–45] and shown in Table 2.

The [1]HNMR spectra of UCO, PGL, and BD are presented in Fig. 6, 7, 8a. The spectrum of UCO illustrates the most important peaks such as terminal $–CH_3$, $–(CH_2)–$ Chain, $β–CH_2$, $–CH_2–CH_2–CH=$, $α–CH_2$,$=CH–CH_2–CH=$, $–CH–CH_2–O(CO)–R$, $–CH_2–CH(CO–R)–CH_2–$, and –CH=CH– at 0.80 ppm, 1.20 ppm, 1.60 ppm, 2.00 ppm, 2.25 ppm, 2.75 ppm, 4.00–4.5 ppm, 5.25 ppm, and

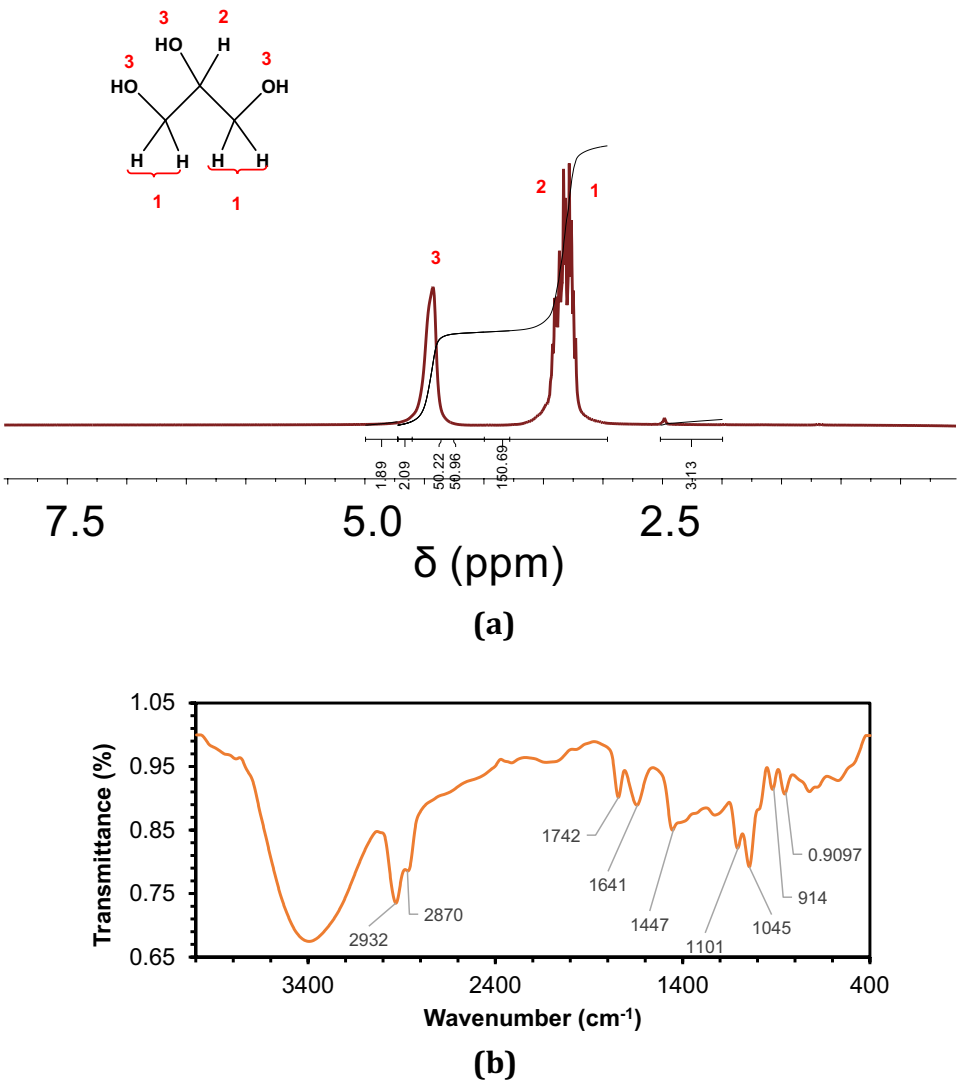

Fig. 9 ^{1}HNMR (**a**) and FTIR (**b**) of commercial glycerol

5.30–5.50 ppm, respectively. Clear differences were observed in both the PGL and BD spectra. For instance, multiple peaks at (a) and one peak at (c) ppm relate to –CH–CH_2–O–H and –CH_2–CH(OH)–CH_2– in the PGL spectrum. More, what distinguishes the spectrum of BD is the strong peak at 3.20 ppm which corresponds to –(CH_2)–, and the peak at 4.20 ppm which corresponds to -OCH_3. When comparing PGL ^{1}HNMR spectrum with ^{1}HNMR spectrum of commercial glycerin, Fig. 9, peaks (1, 2, and 3) are identical and represent the protons of a single molecule of glycerol or linear polyglycerol. The (4) peak may represent the proton attached to the carbon atom that is part of R. The high area of the (4) peak indicates the presence of a significant amount of branching structures.

The PGL and BD were detected in UCO vs. PGL & BD FTIR spectra, Fig. 6, 7, 8b. The intensity of peak in the UCO spectrum at ~ 3001 cm^{-1} corresponded to C-H of alkene, -CH_3 asymmetrical stretching at ~ 2930 cm^{-1} and symmetrical bending at ~ 1370 cm^{-1}, -CH_2 asymmetrical stretching at ~ 2850 cm^{-1}, and scissoring at 1455 cm^{-1}. In addition, a strong peek at ~ 1740 cm^{-1} because of C = O ester stretching vibrations, a small peak at 1655 cm^{-1} relates to C=O free fatty acids, bending of C–O bands at 1250, 1155, 1078 cm^{-1}, and –$(CH_2)_n$- rocking at ~ 714 cm^{-1}. As for the BD spectrum, a broad hydroxyl band appeared at 3383 cm^{-1}, which may be due to the presence of moisture. A peak at ~ 1640 cm^{-1} corresponded to C=O, a strong peek at 1018 cm^{-1}, and peaks appeared at 1466 cm^{-1} related to C–O and CO–O-CH_3 which indicated that the methyl esters are formed. The PGL FTIR spectrum was obtained in the Fig. 8-b. There is a -CH asymmetrical stretching peak at ~ 2930 cm^{-1} and a –(COH) small peak at ~ 1450 cm^{-1}. There is a strong peak in ~ 1641 cm^{-1} may be due to the C=O bond indicating the presence of mono- and diacyl glycerides. Hence, a broad hydroxyl band of glycerol appeared at 3400 cm^{-1}.

The ^{1}HNMR spectra illustrated some changes in the signals. The emergence of new areas in the range of

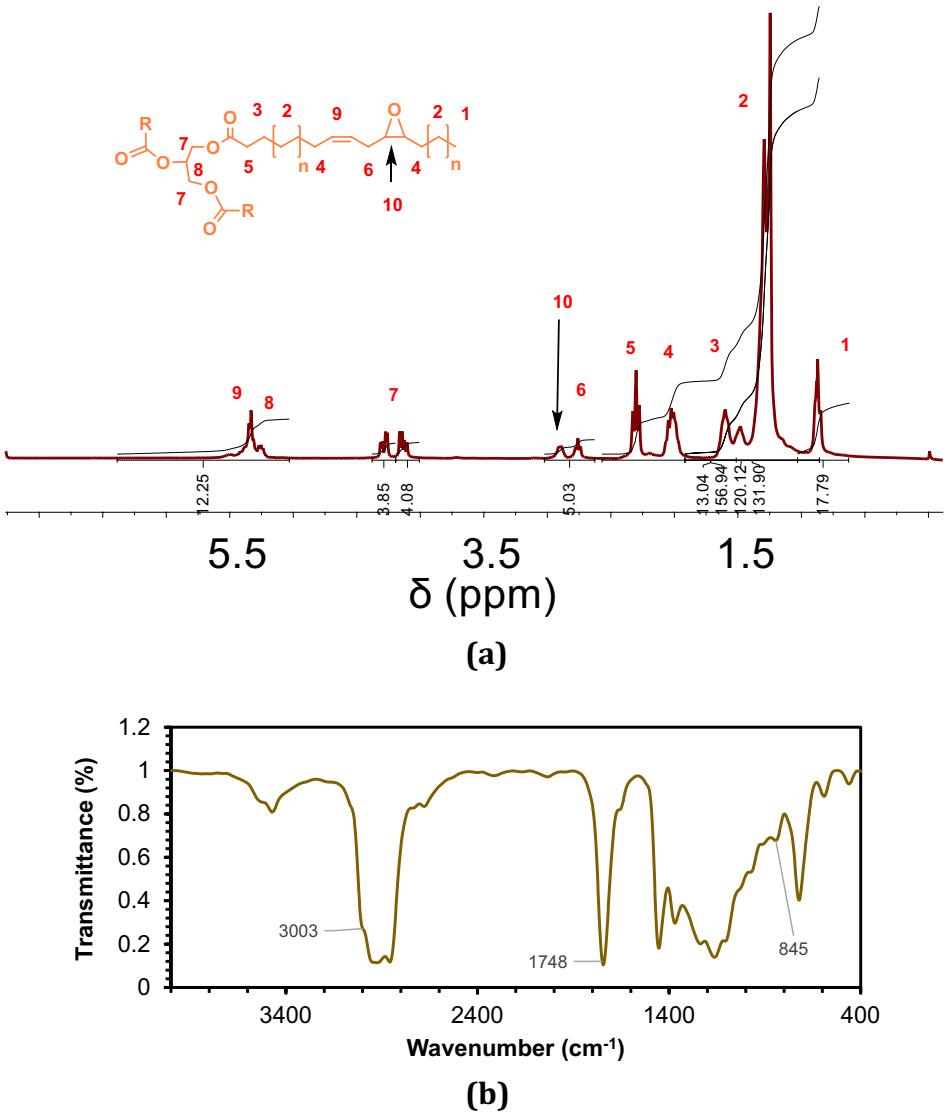

Fig. 10 ^{1}HNMR (**a**) and FTIR (**b**) of EUO

2.80–3.00 ppm belonging to the hydrogens attached to the oxirane ring in the spectrum of EUO coincided with the partial disappearance of some others in the range of 5.30–5.50 ppm belonging to the olefinic hydrogens in the spectrum of UCO. On the other hand, the same areas of 2.80–3.00 ppm disappeared completely to show new ones in the range of 3.40–4.40 ppm in the biopolyols' spectrum. In biopol-PET, the signal at 4.50 ppm corresponded to hydrogens of diethylene glycol, and the signal at 8.15 ppm related to hydrogens of the aromatic cycle of PET. In contrast, weak signals at 6.25–8.25 ppm are derived from the hydrogens of aromatic cycle isocyanate in PU. Likewise, peaks at 6.50–7.50 ppm in the biopol-BPA are caused by the aromatic cycle of BPA, Figs. 10, 11, 12, 13, 14a.

The EUO and biopolyols were detected in FTIR spectra Fig. 10, 11, 12, 13, 14b. The intensity of peak in UCO spectrum at ~ 3001 cm^{-1} corresponded to C–H of alkene was decreased and disappeared in the EUO spectrum, accompanied by appearing a peak at ~ 840 cm^{-1} corresponding to oxirane ring. Generally, there are participated peaks such as a broad hydroxyl band appeared at 3400 cm^{-1} and C=O stretching vibrations at ~ 1700 cm^{-1} in all novel biopolyols' spectra. More, the peek corresponded to the epoxide cycle was faded. The absorption bands at 1000–1200 cm^{-1} correspond to the aliphatic ether group of diethylene glycol. The bending vibrations of the methylene groups in the biopolyol chain are also consistent at 1350–1450 cm^{-1}. The CH bonds in the aliphatic carbon are stretched at 2900–2800 cm^{-1}. Some additional signals appeared such as ~ 1500 cm^{-1} due to aromatic C=C stretching in biopol-PET and biopol-BPA, ~ 1500 cm^{-1} and ~ 1600 cm^{-1} related to amine groups in biopol-PU. [46–49].

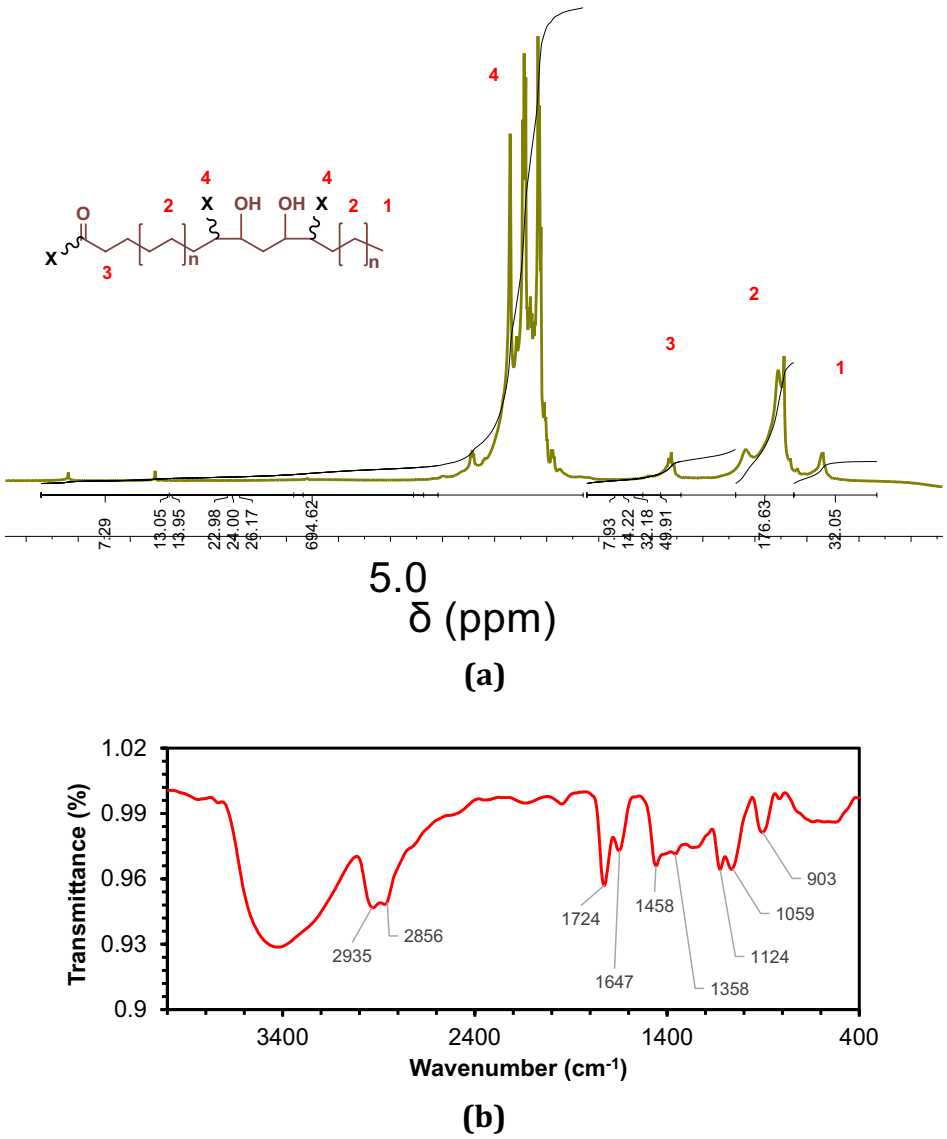

Fig. 11 ^{1}HNMR (**a**) and FTIR (**b**) of biopol-B

3.2 Characterization of polyurethane rigid foams

The foam during formation usually goes through steps where the mixture turns first into a cream and then into a gel, accompanied by the rise of the mixture and the formation of foam. The stirring, cream, gel, and rise times were determined for foams and their composites. The results show that the blend of biopol-BPA takes more time in rise operation. While the values are close for other biopolyols. The reason can be attributed to the type of polyol where the reaction with biopol-BPA takes more time than other types because of high viscosity. The apparent density of foams directly depends on the viscosity of the mixture of components as high viscosity inhibits cell growth. On the other hand, viscosity is related to the degree of compatibility between these components. It can be seen that the apparent density gradually increases with the increase in the biopolyol content for all biopolyols, Table 3, [50–53].

The thermogravimetric analysis is one of the useful methods used for analyzing the thermal degradation of polymers, especially polyurethane rigid foams and their composites. The curves of weight loss (TG) and weight loss derivatives (DTG) in the air atmosphere present in Fig. 15, while the results are summarized in Table 3. Generally, changes on polyurethane foams occur after a temperature of 100 °C. Initially, the hydrogen bonds between the urethane groups and the oxygen atoms of the soft parts and the allophanates and urea bonds are broken within the range 100–180 °C. The main urethane bonds break after 200 °C degrees to destroy the rigid part at 250 °C. Heat breaks urethane bonds with the type of substituents (aliphatic or aromatic) located on both terminals of the urethane group where the urethane groups

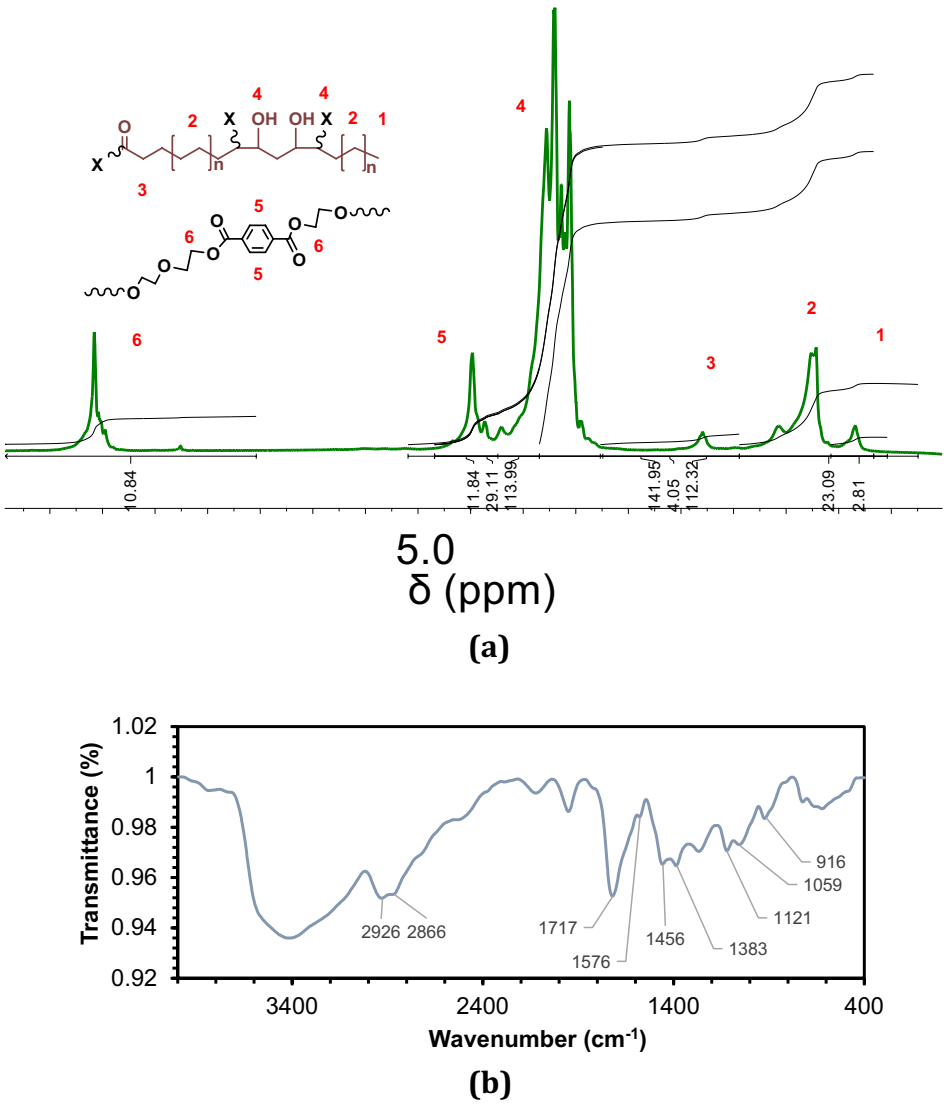

Fig. 12 ^{1}HNMR (**a**) and FTIR (**b**) of biopol-PET

with aliphatic substituents are the most resistant to thermal cracking. This is followed by the decomposition of the soft parts and then the ester groups in the soft parts.

The curves showed two main steps, the first between 180 °C and 430 °C and the second between 430 °C and 700 °C, corresponding to ~ 45% and ~ 55% mass loss, respectively. The first step refers to the degradation of the hard segments including many kinds of bonds and perhaps the most important of which is urethane bonds, which start to break down first, and ester bonds in the soft parts, which start to break down starting from 380 °C. The second step may refer to the decomposition of flexible segments, aromatic compounds or thermolysis of organic residues. Each has a maximum degradation rates T_{max2} = 346–357 °C and T_{max3} = 570–598 °C for based-biopol-B PURFs, T_{max2} = 346–354 °C and T_{max3} = 584–586 °C for based-biopol-PET PURFs, T_{max2} = 317–356 °C and T_{max3} = 584–586 °C for based-biopol-PU PURFs, and T_{max2} = 286–373 °C and T_{max3} = 577–610 °C for based-biopol-BPA PURFs.

The introduction of biopolyols significantly affected the temperature at the beginning of the decomposition $T_{5\%}$ compared with the comparative sample, as it caused a decrease in the temperature for all based-biopolyols PURFs at all ratios except for based-biopol-PU&BPA PURFs at ratio 20% $PU_{\_PU\text{-}20}$ and $PU_{\_BPA\text{-}20}$, which have increased. The decrease was notable for all foams with ratio 60% $PU_{\_com\text{-}60}$, $PU_{\_PET\text{-}60}$, $PU_{\_PU\text{-}60}$, and $PU_{\_BPA\text{-}60}$. The introduction of biopol-B, PET, PU, and BPA at ratio 60% for the fabricated foams led to some changes in the foam structure and observation of an additional step in the thermal decomposition corresponding to the degradation of the rigid segments T_{max1}. As the biopolyol content increases 40%, 60%, the degree of phase separation in polyurethane foam increases. Probably, causes the pyrolysis pathway of the foam to be changed to form a three-phase state which

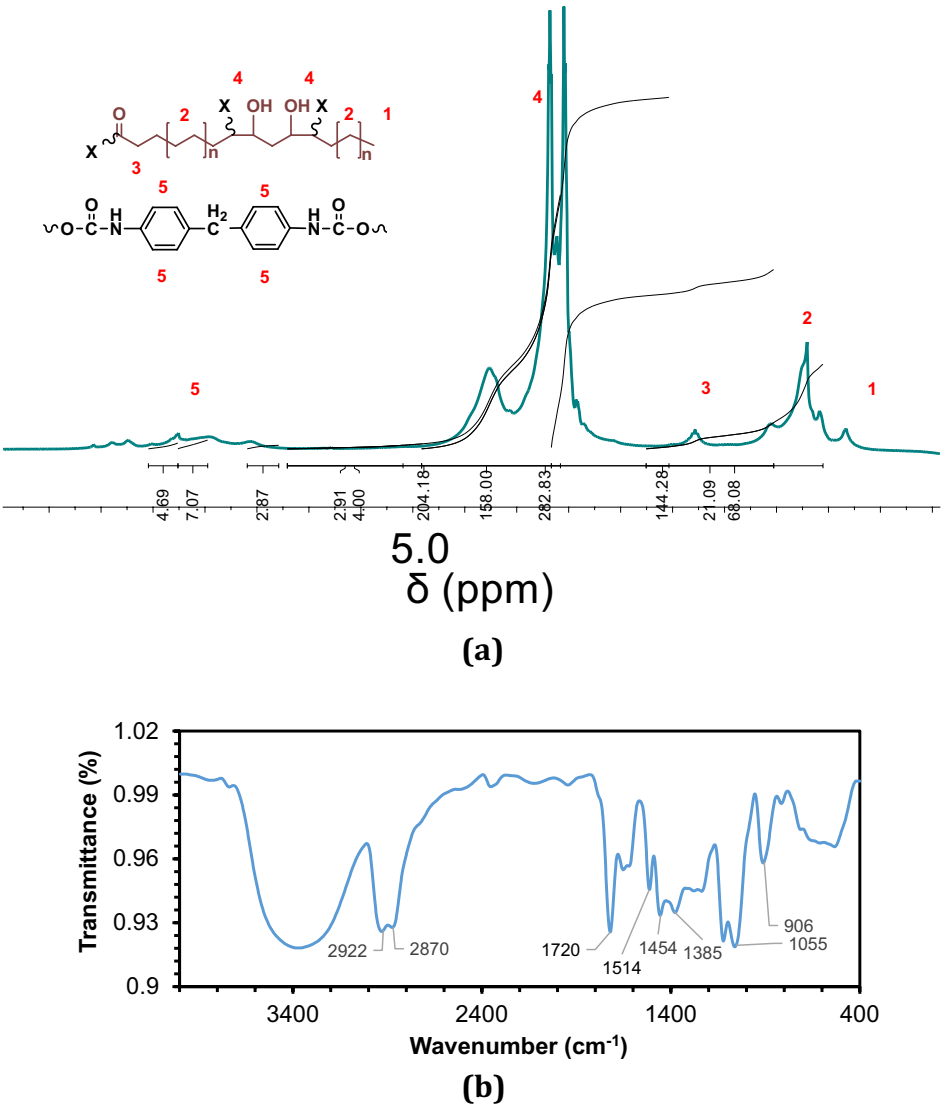

Fig. 13 ^{1}HNMR (**a**) and FTIR (**b**) of biopol-PU

results in a 10% and 20% reduction in weight loss of $PU_{\_B\text{-}60}$, $PU_{\_PET\text{-}60}$, $PU_{\_BPA\text{-}40\ \&\ 60}$, and $PU_{\_PU\text{-}60}$, respectively. The results of the analysis, when compared with the reference sample, indicate sometimes higher or equal thermal stability for foams $PU_{\_B\text{-}40}$, $PU_{\_PET\text{-}40}$, and $PU_{\_PU\text{-}20}$, and sometimes less for other foams, as evident from the values of the table at the 50% mass loss temperatures. The values of V_{max} from the curves for the first decomposition steps show that the decomposition speed of the reference sample is slower than the rest of the samples, but at the middle and last steps, it shows a different behavior as it becomes faster except for foams $PU_{\_PET\text{-}60}$, $PU_{\_BPA\text{-}60}$. The percentage of combustion residues at 800 °C has no significant effect for foams after the introduction of biopolyols [54–60].

The changes which occurred in the morphology of cellular structures of foams because of blending of the reference sample with biopolyols which was depicted by SEM, Figs. 16, 17, 18, 19, 20. The different behavior can be attributed to the different reactions of biopolyols according to different weight ratio as it is considered a hydrophilic and hydrophobic functional groups container material, which affects the morphological and structure of the pores including cracks in the walls, collapse, and deform at the largest weight percentage. The cells of most of the images show oval shapes and wide range of sizes. More, comparison sample $PU_{\_com}$ image shows an average diameter 287 ± 140 µm.

The introduction of biopol-B by weight ratios of 20, 40, and 60% for samples $PU_{\_B\text{-}20}$, $PU_{\_B\text{-}40}$, and $PU_{\_B\text{-}60}$ has led to a gradual increase in the average cells' diameter to be 353 ± 103, 339 ± 103, and 313 ± 92 µm, respectively. The sample of $PU_{\_B\text{-}60}$ has some deformation, Fig. 17c. The addition of biopol-PET for samples $PU_{\_PET\text{-}20}$, $PU_{\_PET\text{-}40}$, and $PU_{\_PET\text{-}60}$ has led to a significant increase in the average pore diameter comparing with $PU_{\_com}$, the increase was gradually by 383 ± 104, 393 ± 120, and 436 ± 220 µm, respectively. The average diameter of the foam cells has

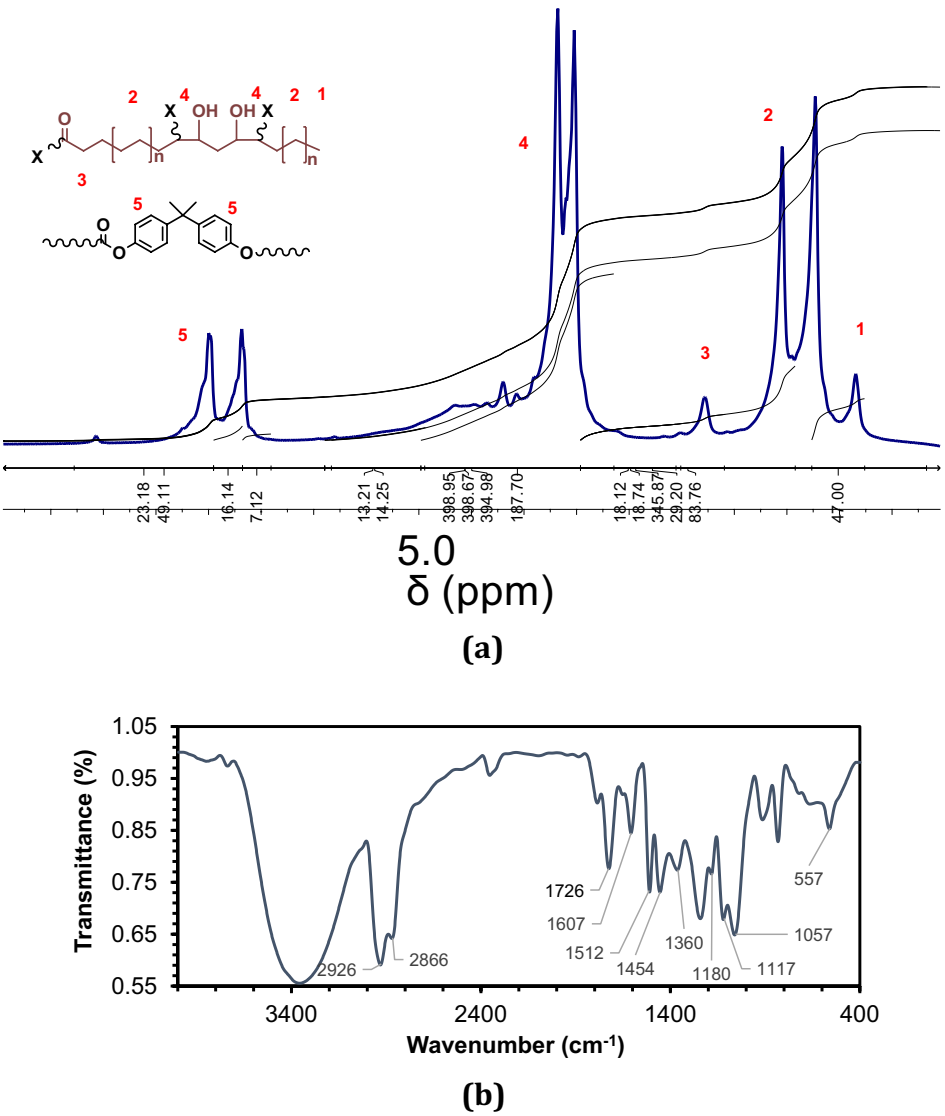

Fig. 14 [1]HNMR (**a**) and FTIR (**b**) of biopol-BPA

increased significantly upon introduction of biopol-PU from 287 ± 140 µm for $PU_{\_com}$ to 495 ± 166 µm, 438 ± 147 µm, and 460 ± 219 for 20%, 40%, and 60%, respectively. The mean values of cell diameters increased slightly when biopol-BPA was added to the comparative sample and ranged between 285 and 334 µm. Nevertheless, it can be seen that the cell density of the blended foams is higher than that of the comparison sample. This can be attributed to the presence of a very small percentage of bubbles or large vacuoles resulting from the fusion of some cells with each other, which led to an increase in the standard deviation of cell diameter in the two samples $PU_{\_BPA\text{-}20}$. This happened in the sample $PU_{_BPA\text{-}60}$but this was accompanied by the collapse and crash of the bubble and this explains the presence of distortions in the structure [61–66].

Dynamic mechanical thermo-analysis (DMTA) is used to study the response of viscoelastic materials to periodic deformation as a function of temperature change. The figures, Figs. 21, 22, represents the loss factor (tan δ), the storage modulus (E'), and the loss modulus (E") of the prepared polyurethane rigid foams. Samples based on the blended biopol-B with commercial polyol show a gradual decrease in the storage modulus with increasing temperature. At 25 °C, a change was observed in the storage factor values for the ratios 20%, 40%, and 60% compared to the reference sample, as it increased for the last mixture other than the first and second blends. The temperature dependence curve of the loss factor shows that the peak value of the loss factor increases with the increase in the content of biopol-B, that is, 60%, while at the two percentages 20%

Table 3 Characterization of foaming process, foam properties, and summary of TGA results of foams

	x	Stirring time (sec)	Cream time (sec)	Gel time (sec)	Rise time (sec)	Apparent density[a] (g/cm^3)	$T_{5\%}$, (°C)	$T_{50\%}$, (°C)	T_{max1}, (°C)	T_{max2}, (°C)	T_{max3}, (°C)	Residue (%)
$PU_{\_x\text{-}20}$	B	6	11	22	35	0.094	236	441	–	357	571	0
	PET	6	11	24	38	0.042	219	483	–	354	585	0
	PU	6	11	24	38	0.040	275	514	–	356	600	0
	BPA	6	12	30	60	0.061	265	449	–	373	577	0
$PU_{\_x\text{–}40}$	B	6	10	23	36	0.095	229	507	–	436	598	0
	PET	6	11	23	38	0.050	227	501	–	353	584	0
	PU	6	11	24	38	0.065	237	469	–	345	585	0
	BPA	6	12	30	61	0.066	90	465	125	337	603	0
$PU_{\_x\text{–}60}$	B	6	12	24	35	0.096	98	482	110	356	581	0
	PET	6	12	24	40	0.064	172	494	190	346	586	0
	PU	6	11	24	38	0.068	94	322	122	317	583	0
	BPA	6	12	31	64	0.075	58	547	89	286	610	0
$PU_{\_com}$		5	10	23	37	0.047	238	501	–	354	584	0

[a]The densities of foams were calculated by using the formula described in DIN 53479[50]

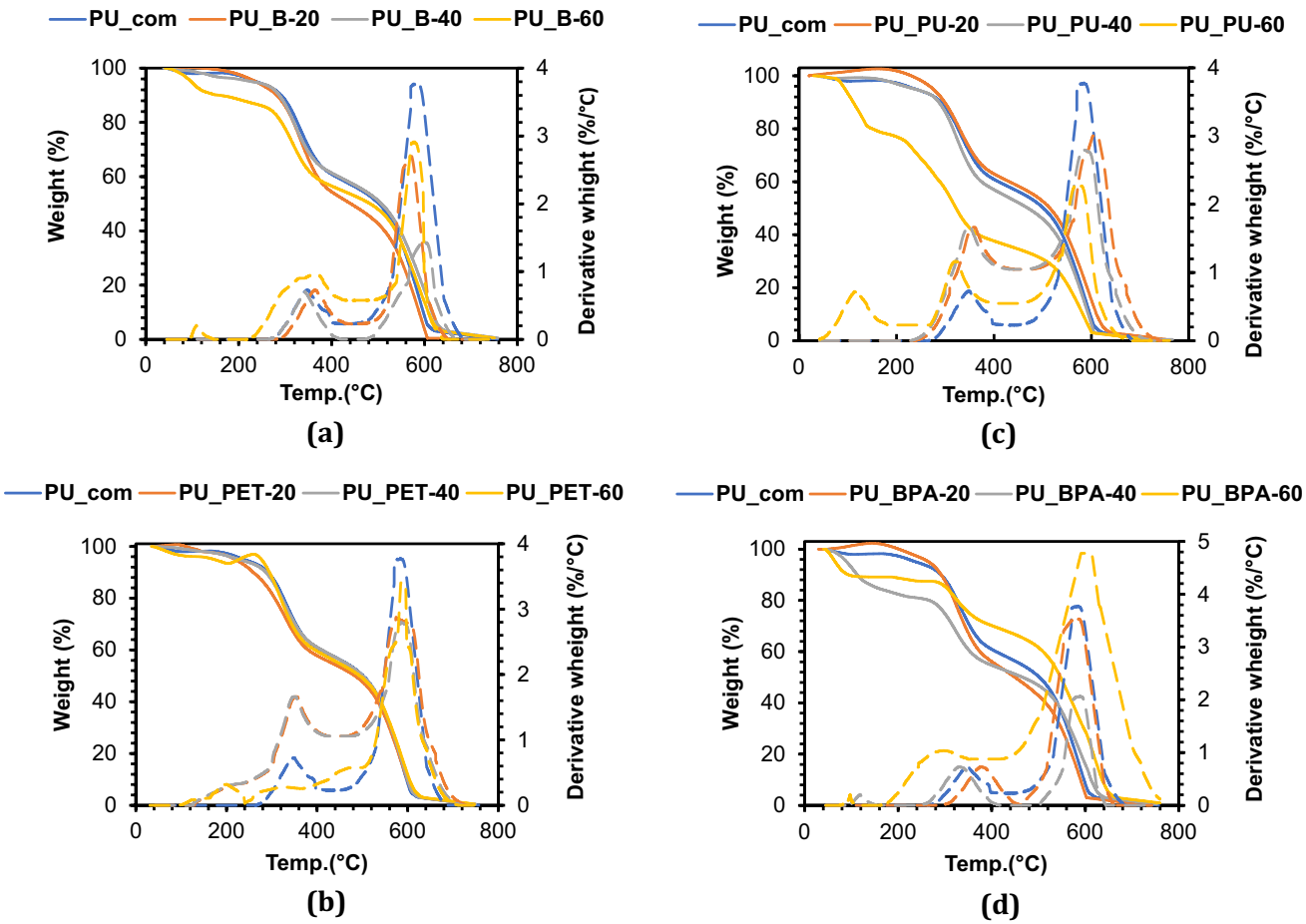

Fig. 15 TGA-DTG of foams based on biopol-B (**a**), biopol-PET (**b**), biopol-PU (**c**), and biopol-BPA (**d**)

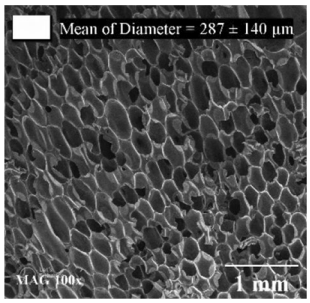

Fig. 16 SEM of comparative foam

and 40%, the values were lower compared to the reference sample. The glass transition temperature was taken from the tan δ_{max} peaks and the values were 209, 215, 197, and 163 °C for samples $PU_{\_com}$, $PU_{\_B\text{-}20}$, $PU_{\_B\text{-}40}$, and $PU_{\_B\text{-}60}$, respectively. It is possible that the addition of a small percentage of biopol-B resulted in better localization of the hydroxyl groups within the polymer matrix to become more available than in the comparison sample. This resulted in more cross-linking points in order to form hydrogen bonds with the isocyanate groups and thus would impede the movement of the polymeric chains or the increase in the solid section and the value of the glass transition. This

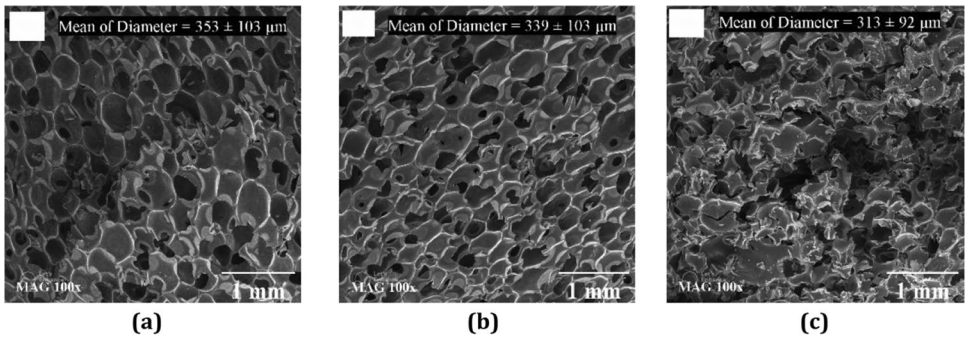

Fig. 17 SEM of foams based on biopol-B: 20% (**a**), 40% (**b**), and 60% (**c**)

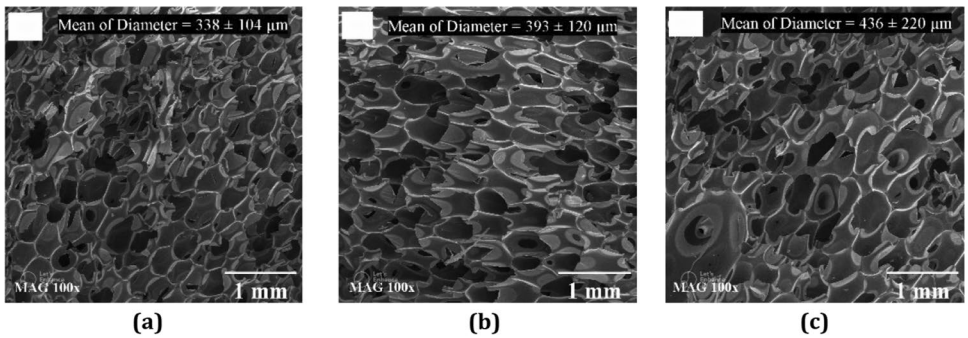

Fig. 18 SEM of foams based on biopol-PET: 20% (**a**), 40% (**b**), and 60% (**c**)

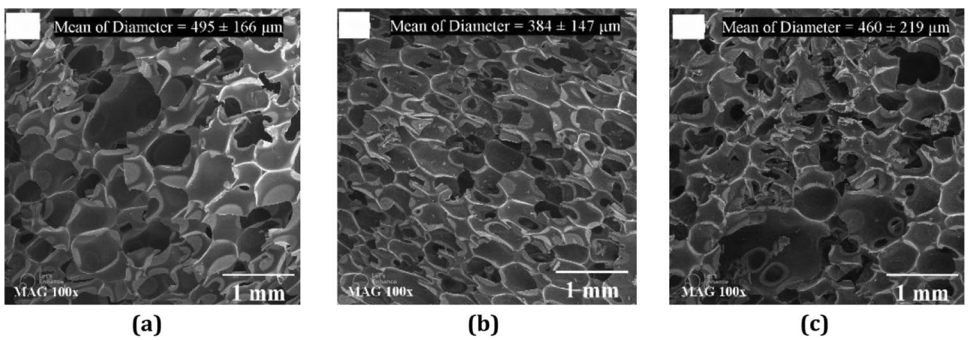

Fig. 19 SEM of foams based on biopol-PU: 20% (**a**), 40% (**b**), and 60% (**c**)

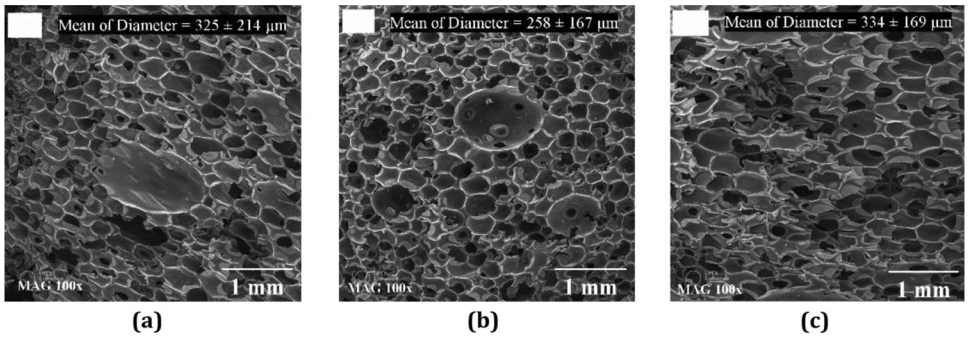

Fig. 20 SEM of foams based on biopol-BPA: 20% (**a**), 40% (**b**), and 60% (**c**)

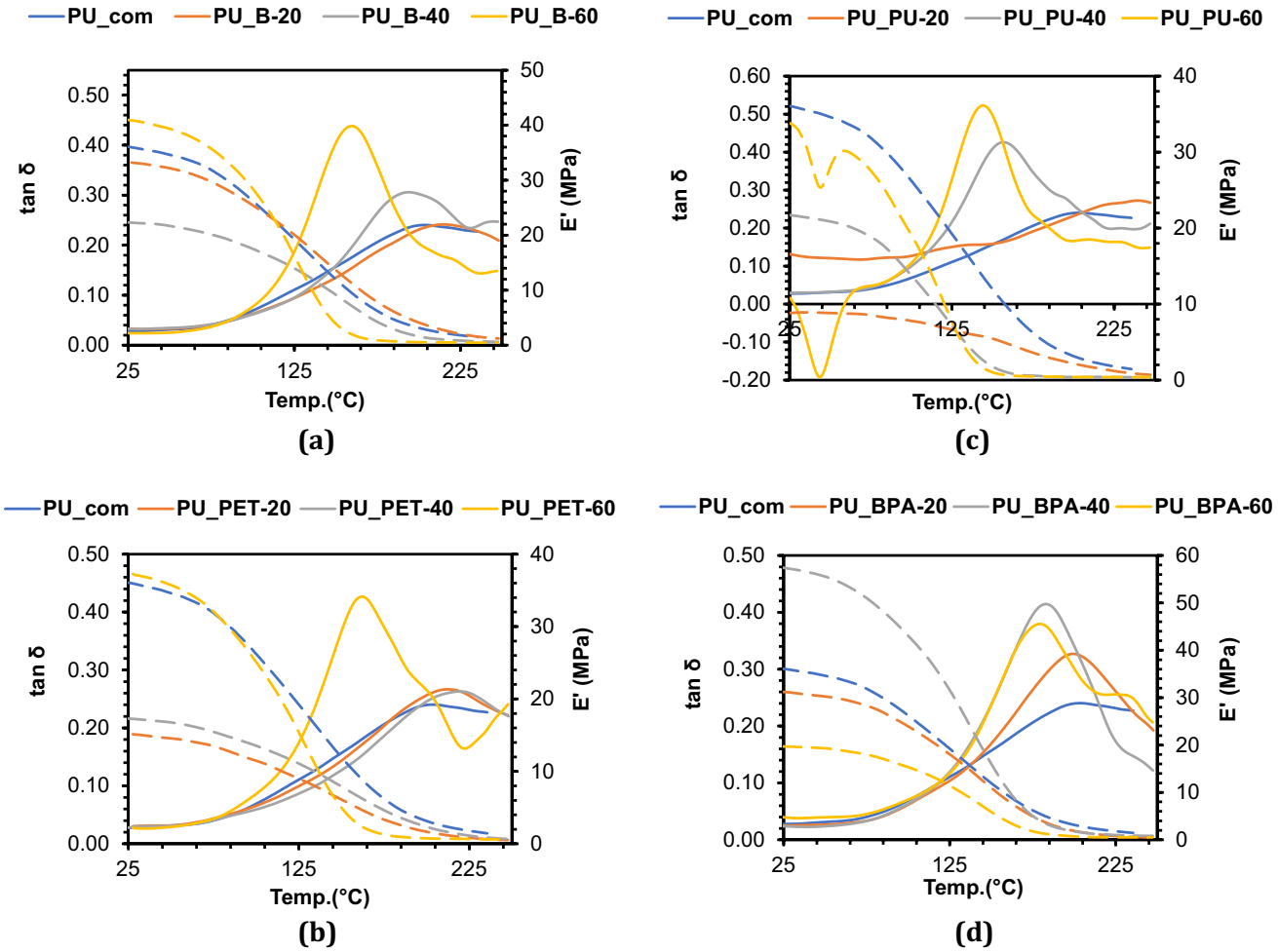

Fig. 21 DMTA-1 of foams based on biopol-B (**a**), biopol-PET (**b**), biopol-PU (**c**), and biopol-BPA (**d**)

confirms that the peak heights of the samples $PU_{\_com}$ and $PU_{\_B\text{-}20}$ are equal, given that the height of tan δ_{max} represents the entanglement density. All samples show only one peak, indicating the homogeneous nature of polyurethane foams. The introduction of biopol-PET on the comparison polyol at the weight ratios of 20% and 40% reduced the storage modulus E' at 25 °C, while no effect occurred at 60%. Also, for the loss modulus E", the peak of $PU_{\_PET\text{-}60}$ was the highest. This behavior is similar to that of biopol-B. The glass transition temperatures of the foams $PU_{\_PET\text{-}20}$ and $PU_{\_PET\text{-}40}$ were almost slightly higher than the blank sample except for the foam $PU_{\_PET\text{-}60}$ which was lower and reached 167 °C. The storage modulus decreased at 25 °C at all ratios when biopol-PU was introduced to the control

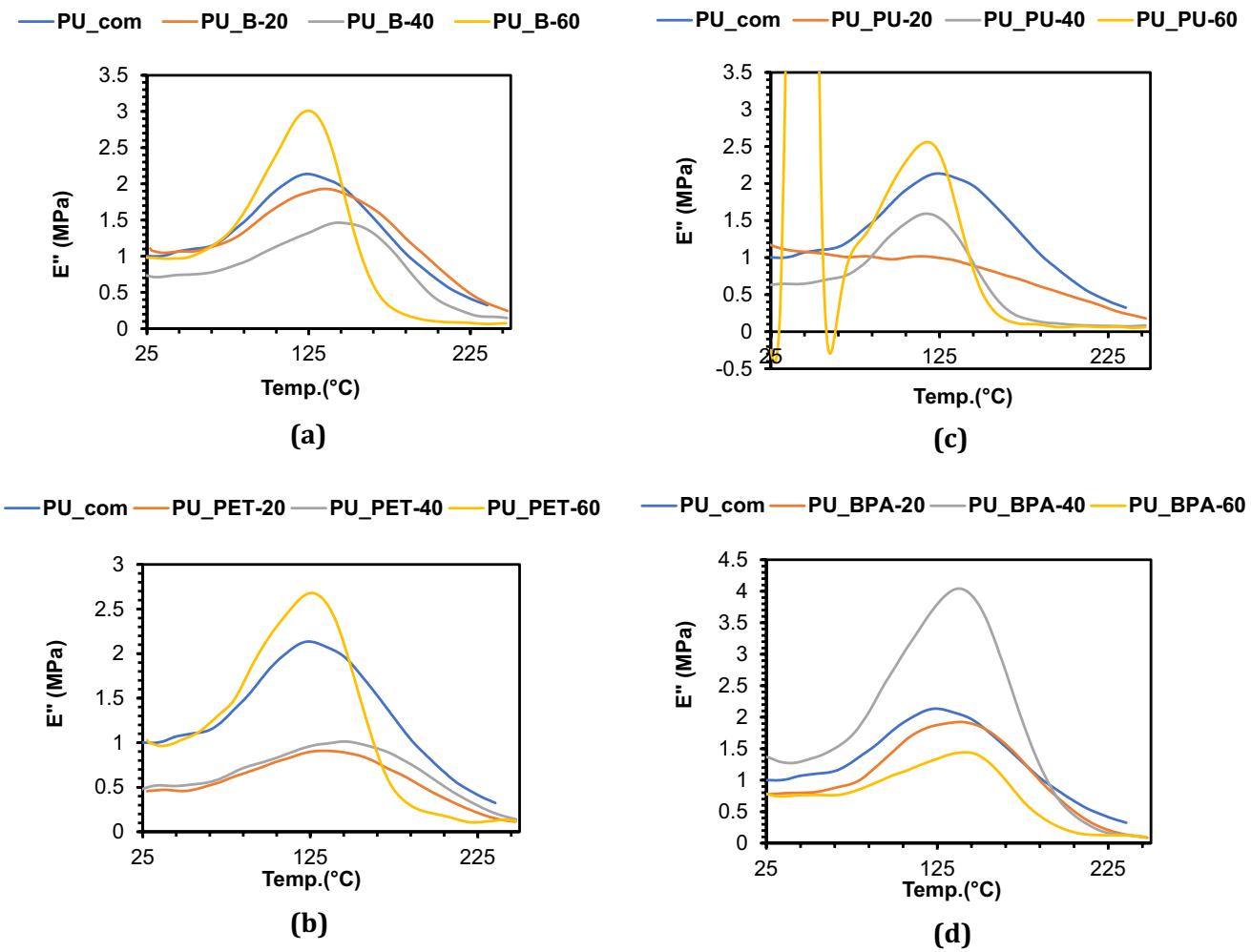

Fig. 22 DMTA-2 of foams based on biopol-B (**a**), biopol-PET (**b**), biopol-PU (**c**), and biopol-BPA (**d**)

polyol. The minimum foam value was at 20 wt%. For the loss modulus, the peak of the $PU_{\_PU\text{-}60}$ foam was the highest. There was a clear difference in the glass transition temperature values for the foams, but two peaks were observed for the $PU_{\_PU\text{-}60}$ foam. This can be attributed to the fact that the presence of a higher proportion of biopolyols resulted in a lack of network integrity due to incompatibility. The storage factor increased at 25 °C for $PU_{\_BPA\text{-}40}$ foam when the biopol-BPA was introduced on the control polyol while the remaining two foams were lower than the control sample. In terms of loss modulus, $PU_{\_BPA\text{-}40}$ foam had the highest peak. The glass transition temperature values for the foams gradually decreased in the tan δ diagram [67–71].

4 Conclusions

The circular economy was achieved by the synthesis of valuable products from 100% wastes through the synthesis of used cooking oil-based biodiesel and polyglycerol. Then, reacting the binary solvent polyglycerol and epoxidized used cooking oil with plastic wastes to achieve the biopolyols.

The properties confirmed by titration methods, rotational rheometer, FTIR, and ^{1}HNMR show obtaining new classes of biopolyols with different hydroxyl numbers and viscosities and may exceed use in polyurethane foaming.

However, the rigid foams are fabricated from mixing novel biopolyols with commercial polyol in specific weight ratios (20%, 40%, and 60%).

The thermal, morphological, and thermo-mechanical properties of rigid foams confirmed by TGA-DTG, SEM, and DMTA show insignificant changes results comparing with the comparative sample at the commercial-industrial level for foams prepared 20% and 40% biopolyol mixtures.

For foams prepared 60%, TGA-DTG, SEM, and DMTA results also show partial deformity in cellular structure and

somewhat different behavior in thermal and mechanical characteristics.

Our work confirms that it is very possible to embody the principle of industrial ecology on the ground, which is to make the waste of one industry the raw material in another industry. Moreover, it is necessary to apply these products in other industries (other than polyurethane foam manufacturing). In addition, testing non-traditional production methods that are more sustainable and environmentally friendly to synthesize such as these valuable materials.

Author contributions The study conception, design, material preparation, data collection, analysis, and the first draft of the manuscript were performed by MS. All authors read and approved the final manuscript.

Funding The authors declare that no funds, grants, or other support were received during the preparation of this manuscript except for some of techniques used in the research located at the university.

Data availability The datasets generated during or analyzed during the current study are available from the corresponding author on reasonable request.

Declarations

Conflict of interest The authors declare no conflict of interests.

References

1. R. Jerome, M. Granville, B. Boutevin, J. Robin. Prog. Polym. Sci **16**(5), 837–906 (1991)
2. G. Woods, *The ICI polyurethanes book* (John Wiley & Sons Ltd, 1987)
3. M. Szycher, *Polyurethanes* (CRC Press, Boca Raton, 2013)
4. M. Buist, J. Grayson, D. Woolley, *Fire and cellular polymers* (Springer Science & Business Media, 2012)
5. M. Ionescu, *Chemistry and technology of polyols for polyurethanes* (iSmithers Rapra Publishing, 2005)
6. F. Carroll, Phys. Sci. Rev **1**, 9 (2016)
7. X. Yi, R. Dong, N. Tang, Constr Build Mater **236**, 117621 (2020)
8. M. Khalaf, H. Tantawy, A. Soliman, M. Abd El-lateef, J. Mol. Struct **1203**, 127442 (2020)
9. M. Kurańska, K. Polaczek, M. Królikowska, A. Prociak, J. Ryszkowska, Polym J **190**, 122164 (2020)
10. S. Samanta, R. Sahoo, Bioenergy Res **14**(1), 163–174 (2021)
11. W. Li, M. Huang, W. Zhao. In IOP Conference Series Earth and Environmental Science Vol. 153, No. 5, p. 052036 (2018)
12. L. Permadani, M. Ibadurrohman. In IOP Conference Series Earth and Environmental Science Vol. 105, No. 1, p. 012036 (2018)
13. Q. Zhang, S. Saleh, J. Chen, Q. Shen, A review. Chem. Phys. Lipids **165**(6), 662–681 (2012)
14. M. Kurańska, J. Banaś, K. Polaczek, M. Banaś, A. Prociak, J. Kuc, T. Lubera, Ind Crops Prod **7**(6), 103506 (2019)
15. M. Kurańska, E. Malewska, Ind Crops Prod **162**, 113294 (2021)
16. M. Kurańska, H. Beneš, A. Prociak, O. Trhlíková, Z. Walterova, W. Stochlińska, J. Clean. Prod **236**, 117615 (2019)
17. A. Shankar, R. Pentapati, K. Prasad, Egypt. J. Pet **26**(1), 125–133 (2017)
18. H. Park, N. Khan, S. Lee, K. Zimmermann, M. DeRosa, L. Hamilton, P. Pursell, ACS Omega **4**(4), 7775–7784 (2019)
19. S. Niju, G. Vishnupriya, M. Balajii, Sustain. Environ. Res. **29**(1), 1–12 (2019)
20. K. Vasić, G. Hojnik, Ž Knez, M. Leitgeb, J. Catal **10**(2), 237 (2020)
21. J. Li, X. Liang, Manag **141**, 126–132 (2017)
22. H. Zhang, H. Li, H. Pan, A. Wang, S. Souzanchi, C. Xu, S. Yang, Appl. Energy **223**, 416–429 (2018)
23. W. Tan, A. Aziz, K. Aroua, Renew. Sustain. Energy Rev. **27**, 118–127 (2013)
24. S. Kongjao, S. Damronglerd, M. Hunsom, Korean J Chem Eng **27**(3), 944–949 (2010)
25. X. Luo, Y. Li, J Polym Environ **22**(3), 318–328 (2014)
26. A. Nikje, F. Abedinifar, A. Appl, Sci. Res **3**, 383–388 (2011)
27. R. Nanda, Z. Yuan, W. Qin, A. Poirier, X. Chunbao, Austin J. Chem. Eng. **1**(1), 1–7 (2014)
28. A. Yusof, Z. Abidin, M. Zailani, K. Govindan, M. Iranmanesh, J. Clean. Prod **121**, 64–71 (2016)
29. P. Benyathiar, P. Kumar, G. Carpenter, J. Brace, K. Mishra, Polymers **14**(12), 2366 (2022)
30. Y. Liu, X.B. Lu, J. Polym. Sci (2022)
31. A. Grigsby, P. Speranza, E. Brennan. USPTO, No. 4,469,824 (1984)
32. L. Yeakey, M. Cuscurida. USPTO, No. 4,468,483 (1984)
33. I. Cano, C. Martin, A. Fernandes, W. Lodge, J. Dupont, A. Carmona, I. Pedro, Appl. Catal. B **260**, 118110 (2020)
34. A. Sheldon, Chem. Ind **23**, 903–906 (1992)
35. N. Azgomi, M. Mokhtary, J. Mol. Catal: Chemical **398**, 58–64 (2015)
36. A. Sheldon, ACS Sustain. Chem. Eng. **6**(1), 32–48 (2018)
37. A. Ivdre, D. Soto, U. Cabulis, J. Renew. Mater. **4**(4), 285–293 (2016)
38. A. Ivdre, A. Fridrihsone-Girone, A. Abolins, U. Cabulis, J. Cell. Plast. **54**(2), 161–177 (2018)
39. A. Ivdre, A. Abolins, I. Sevastyanova, M. Kirpluks, U. Cabulis, R. Merijs-Meri, J. Polym. **12**(4), 738 (2020)
40. L. Pisarello, O. Dalla Costa, S. Veizaga, A. Querini, Ind. Eng. Chem. Res **49**(19), 8935–8941 (2010)
41. Malroptseva, *Laboratory practice in chemistry and technology of macromolecular compound* (Khemya Mosco, 1972)
42. H. Allen, B. Sitholé, M. MacLeod, L. Lapointe, J. McPhee, J. Pulp Paper Sci **17**(3), J85–J91 (1991)
43. F. Longman, The analysis of detergents. Talanta **22**(8), 621–636 (1975)
44. I. Doudin, FUELAC **284**, 119114 (2021)
45. K. Kainthan, B. Muliawan, G. Hatzikiriakos, E. Brooks, Macromolecules **39**(22), 7708–7717 (2006)
46. S. Cassel, C. Debaig, T. Benvegnu, P. Chaimbault, M. Lafosse, D. Plusquellec, P. Rollin, EurJOC **5**, 875–896 (2001)
47. G. Vlahov, Nucl. Magn. Reson. Spectrosc **4**(35), 341–357 (1999)
48. A. Prociak, Cell. Polym **26**(6), 381–392 (2007)
49. A. Prociak, Polimery **53**, 3 (2008)
50. J. John, M. Bhattacharya, B. Turner, J. Appl. Polym. Sci **86**(12), 3097–3107 (2002)
51. V. Somisetti, S. Allauddin, R. Narayan, N. Raju, JCTR **15**(1), 199–210 (2018)
52. A. Yadav, M. de Souza, T. Dawsey, K. Gupta, Ind. Eng. Chem **61**(41), 15046–15065 (2022)
53. P. Florian, K. Jena, S. Allauddin, R. Narayan, N. Raju, Ind. Eng. Chem **49**(10), 4517–4527 (2010)
54. V. Somisetti, S. Allauddin, R. Narayan, N. Raju, RSC Adv. **5**(90), 74003–74011 (2015)
55. D. Favero, R. Marcon, T. Barcellos, M. Gómez, J. Sanchis, M. Cars, O. Bianchi, J. Mol. Liq. **285**, 136–145 (2019)
56. S. Shoaib, Asian J. Appl. Sci **2**, 5 (2014)

57. L. Antonio, F. Juan, Polym. Degrad. Stab **91**(2), 221–228 (2006)
58. D. Simón, M. Borreguero, A. De Lucas, F. Rodríguez, Polym. Degrad. Stab **109**, 115–121 (2014)
59. J. Krupers, F. Bartelink, J. Grünhauer, M. Moller, Polym J. **39**(10), 2049–2053 (1998)
60. A. Paberza, A. Fridrihsone-Girone, A. Abolins, U. Cabulis, Polym. J. **60**(9), 572–578 (2015)
61. F. Malak, A. Anderson, IJMS **47**(6), 867–883 (2005)
62. C. Gomez, R. Zakaria, M. Aung, N. Mokhtar, B. Yunus, J. Mater. Res. Technol **9**(6), 16303–16316 (2020)
63. A. Hejna, J. Haponiuk, Ł Piszczyk, M. Klein, K. Formela, E-Polymers **17**(5), 427–437 (2017)
64. A. Prociak, M. Kurańska, E. Malewska, Polimery **62**, 353 (2017)
65. A. Prociak, M. Kurańska, U. Cabulis, J. Ryszkowska, M. Leszczyńska, K. Uram, M. Kirpluks, Ind. Crops Prod. **120**, 262–270 (2018)
66. T. Yang, S. Zhao, L. Dai, Y. Fu, Q. Lin, J Polym Environ **20**(1), 230–236 (2012)
67. V. Gama, B. Soares, S. Freire, R. Silva, P. Neto, A. Timmons, A. Ferreira, Mater. Des **76**, 77–85 (2015)
68. C. Zhang, A. Madbouly, R. Kessler, ACS Appl. Mater. Interfaces **7**(2), 1226–1233 (2015)
69. S. Tan, T. Abraham, D. Ferenc, W. Macosko, Polym J **52**(13), 2840–2846 (2011)
70. R. Chen, C. Zhang, R. Kessler, J. Appl. Polym. Sci **132**, 1 (2015)
71. C. Zhang, R. Ding, R. Kessler, Macromol. Rapid Commun **35**(11), 1068–1074 (2014)